JMEPEG (2009) 18:79–82
DOI: 10.1007/s11665-008-9261-1

1059-9495/$19.00

Microstructure and Mechanical Properties of Multicomponent Aluminum Alloy by Rapid Solidification

C. Li, D.Y. Li, J.C. Li, and Q. Jiang

(Submitted September 3, 2007; in revised form May 19, 2008)

$Al_{90}Ni_{2.5}Ti_{2.5}La_{2.5}Mn_{2.5}$ alloy with multicomponent alloying elements was prepared by rapid solidification. The hardness and the compression strength of the alloy reached 285 HV and 712 Mpa, respectively. The alloy exhibited good wear resistance, which was three times that of the conventional A309 aluminum alloy. The high strength and wear resistance of the alloy were attributed to the second-phase strengthening and the solid solution strengthening mechanisms.

Keywords aluminum alloy, mechanical property, microstructure

1. Introduction

Considerable efforts had been devoted to the development of novel lightweight engineering materials during the last decades. Aluminum alloys had received considerable attention especially in automobile and aerospace industries due to their high specific strengths. To further increase the strength of conventional crystalline aluminum alloys with good ductility, rapid solidification methods (RS) and mechanical alloying methods (MA) had been successfully utilized to decrease grain size, to increase solid solubility and to obtain amorphous matrix (Ref 1-8). Al-Ln-TM (Ln = rare earth, Tm = V, Cr, Mn, Fe, Mo) amorphous aluminum alloys of melt-spun ribbons possessed high strength (Ref 8-11). The tensile strengths of the amorphous aluminum alloys were more than 1000 MPa (Ref 9). If α-Al nanoparticles or icosahedral quasicrystals were embedded in amorphous matrix with coherent interfaces, the strength of the alloy was further improved (Ref 10-17). The strength of the alloys could be further increased by the precipitation of nanoscale Al particles in the amorphous matrix. For example, Choi et al. had reported tensile fracture strengths as large as 1980 MPa for an amorphous alloy containing 18% Al nanocrystals; this strength was about 1.6 times larger than for the fully amorphous alloy (Ref 18). The precipitation of nanoscale Al particles in rapidly solidified amorphous Al-Ni-Ce, Al-Ni-Cu-Ce, Al-Ni-Zr (Ref 19), and Al-Ni-Y (Ref 20) alloys had been reported. Although these ribbons exhibited ultimate strengths exceeding the performance of conventionally produced Al-alloys by a factor of two to three, they could not be directly utilized as structural materials due to their small size. Powder metallurgy technique (P/M) and spark plasma sintering method (SPS) were recently used to fabricate bulk samples (Ref 21-24). The mechanical properties, such as strength, plasticity, and wear resistance, of AlMnCe and AlLaNi alloys prepared by P/M and SPS were reported (Ref 21-25); the strengths of the bulk alloys could reach 800-950 MPa. But the fabrication of bulk high-strength aluminum alloys by P/M and SPS needed high pressure and temperature as compared with other methods. Furthermore, the porosity of the fabricated alloys was avoided with difficultly. Recent researches indicated that by adding multicomponent alloying elements (Ref 25-28), the strength of the alloys were improved. Based on the thermodynamic principle, a new alloy design concept, "multi-principle-element alloy," was explored by Yeh J. W. et al., which was named as high entropy (HE) alloy and mainly consists of simple fcc or bcc solid solution phases (Ref 25-28). HE alloys as multicomponent alloys were composed of n major alloy elements with $n \geq 5$ in equimolar or near-equimolar ratios. This leads to an increase in the stability of the solution due to maximizing the mixing entropy.

Based on above consideration, in this contribution, the high-strength aluminum alloy with multicomponent alloying elements was fabricated by rapid solidification, and the properties and the microstructure of the alloys were investigated.

2. Experimental Procedures

The starting materials were made of Al, La, Mn, Ni, and Ti with purities of 99.9% and were melted together in a vacuum induction furnace under argon atmosphere. After melting, the molten alloy was injected into the copper mold with 6 mm diameter and 12 cm length under an applied pressure of 3×10^5 Pa; the cooling rate was about 10^4 K/s. The composition of the alloy was $Al_{90}Ni_{2.5}Ti_{2.5}La_{2.5}Mn_{2.5}$ (at.%). The stress-strain curve of the alloy was measured using an 810 Material

C. Li, J.C. Li, and **Q. Jiang**, Key Laboratory of Automobile Materials, Ministry of Education, Jilin University, Changchun 130025, China; **C. Li, J.C. Li,** and **Q. Jiang**, Department of Materials Science and Engineering, Jilin University, Changchun 130025, China; and **D.Y. Li**, Department of Control Science & Engineering, School of Communication Engineering, Jilin University, Changchun 130022, People's Republic of China. Contact e-mail: ljc@jlu.edu.cn.

Test System (MTS) at a crosshead rate of 0.2 mm/min. The wear resistance was measured using a MG2000 pin-on-disc wear testing machine at room temperature; the loading range was between 10 and 60 N, and the wear time was 10 min with a rotating speed of 200 r/min. The alloy was used as pin material with 6 mm diameter and 10 mm height; the disc was made of 5CrNiMo steel. Before and after the test, the pin was cleaned with ethanol and weighed to measure the weight loss. The weight loss of the samples in the wear test was measured by use of a photoelectric balance with a precision of 0.01 μg. The micro-hardness was measured by an HV-1000 micro-hardness tester under a load of 200 g and a loading time of 15 s. The phase structure analysis of the alloy was made by X-ray diffractometer. The microstructures of the alloys were observed by optic microscope (OP) and field emission scanning electron microscopy (FESEM), and the fracture and worn surfaces were observed by scanning electron microscopy (SEM).

3. Results and Discussion

Figure 1 shows the microstructures of $Al_{90}Ni_{2.5}Ti_{2.5}La_{2.5}Mn_{2.5}$ alloy. The results exhibit a fine lamellar microstructure that is similar to pearlite in steel; the average lamina width is about 0.2 μm. The X-ray results show that the microstructure of the alloy consists of α-Al solid solution, La_3Al_{11}, Al_3Ni_2, and $Al_{19}Mn_4$ intermetallic compounds (see Fig. 2). Generally, Ti is prone to formation of intermetallic compounds with Al, but Ti exists in α-Al solid solution and does not form a compound with Al element in the present results; it may be due to the fact that La reacts with Al and forms a compound prior to Ti. The effect of Ti on the formation mechanism of intermetallic compound in AlNiTiLaMn alloy needs further investigation. The appearance of the above compounds should contribute to the hardness and the strength of the alloy. Thus, the alloy possesses high hardness; the hardness of the alloy reaches 285 HV, which is two times as high as 128 HV of traditional aluminum alloy A309 alloy. Figure 3 illustrates the stress-strain curves of the alloy. The $\sigma_{0.2}$ (the strength of the alloy for 0.2% plastic deformation) and σ_{max} (maximal compression strength of the alloy) are 595 and 712 Mpa, respectively. The fracture surface shown in Fig. 4 exhibits a brittle fracture mode.

The variations in coefficient of friction and wear rate with load for conventional A 309 aluminum alloy and the experimental alloy are shown in Fig. 5. It is noticeable that the effect of load on coefficient of friction is evident, the friction

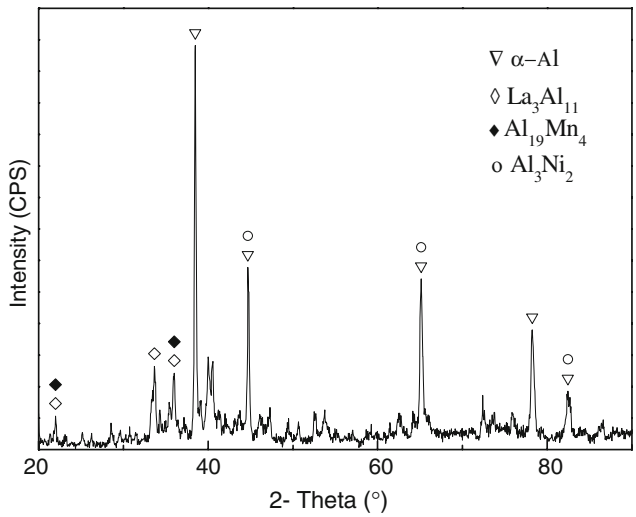

Fig. 2 X-ray analysis of the alloy

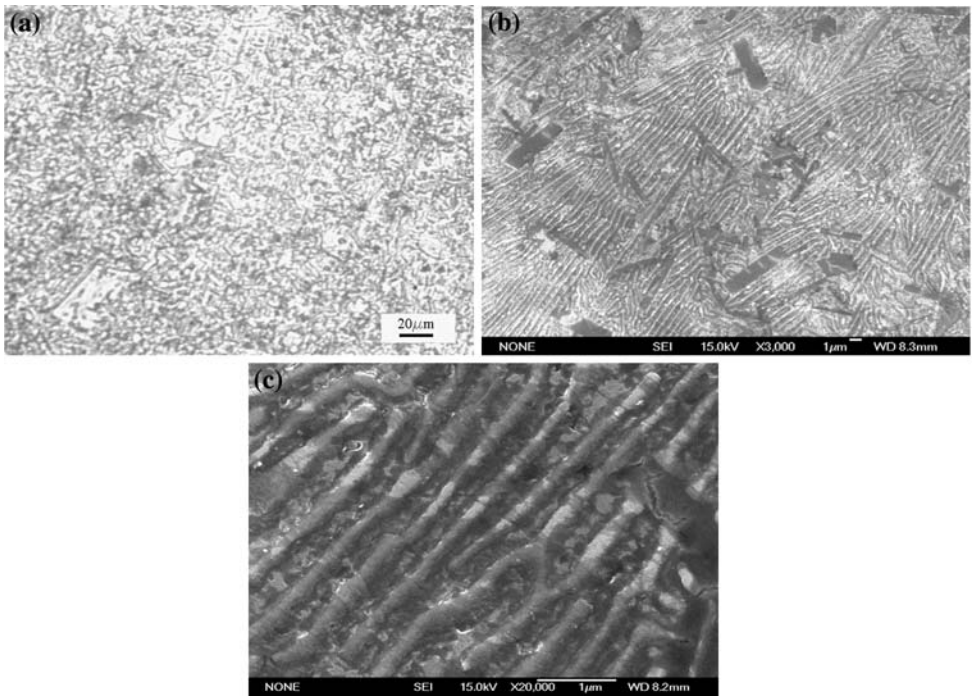

Fig. 1 Micrograph of the alloy. (a) OP, (b) and (c) FESEM

coefficient decreases considerably with increasing load, and the lowest levels in coefficient of friction curve clearly occurred in a load range of 50-70 N. The coefficient of friction of experimental alloy is smaller than that of A 309 aluminum alloy. The excellent strength of the alloy may be accompanied by high wear resistance. The experimental alloy presents improved wear resistance as compared with conventional A 309 aluminum alloy; the results show that there is little difference in the wear resistance for the experimental alloy and conventional A 309 alloy at 10 and 20 N load, because at low load the wear mechanism of the alloys is mainly oxidative wear, and the oxidative layer on the worn surface separates the studied alloy and the wear disc from metal to metal contact. As the load is increased, the plastic deformation on the worn

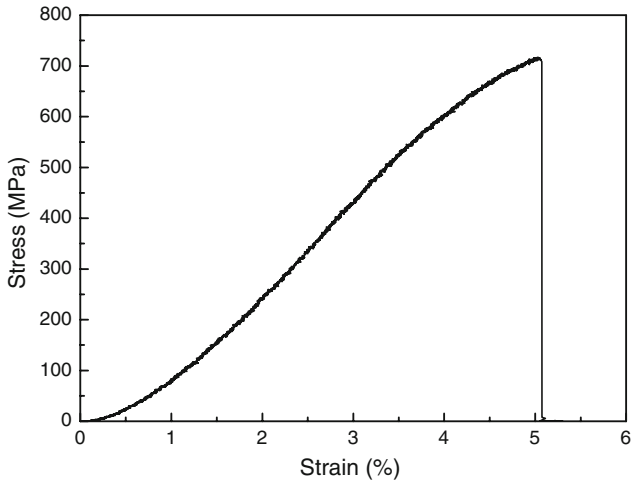

Fig. 3 Stress-strain curve of the alloy

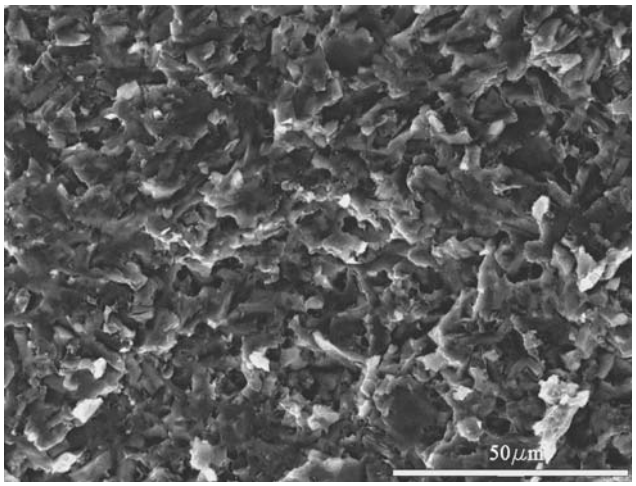

Fig. 4 SEM micrograph of fracture of the compressed sample

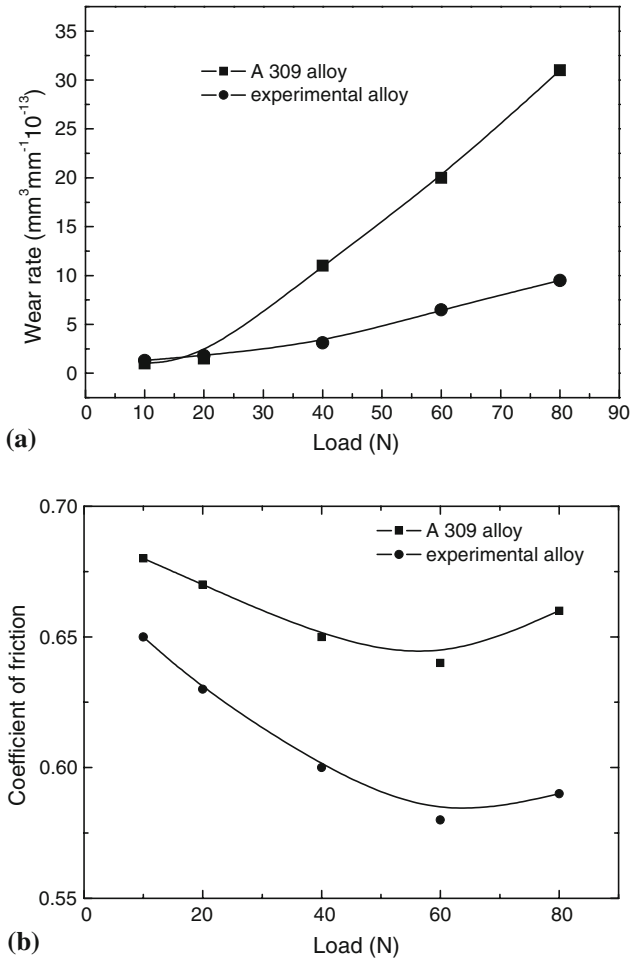

Fig. 5 Wear rate and coefficient of friction curves for the alloys under different loads. (a) Wear rate, (b) coefficient of friction

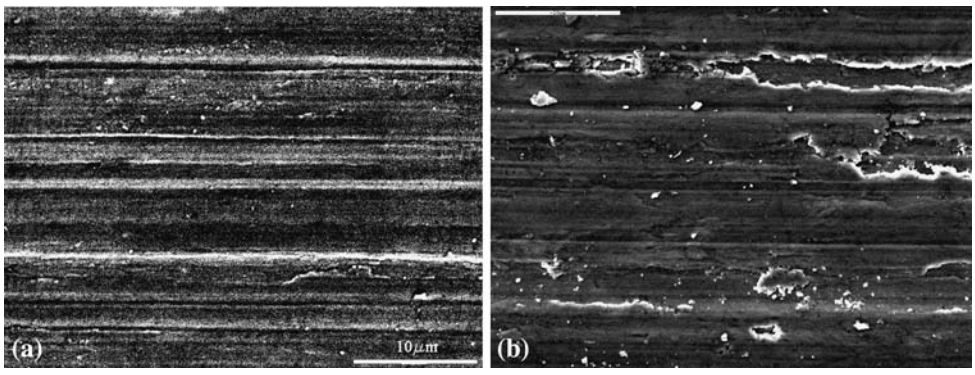

Fig. 6 SEM micrograph of the worn surface of the alloys at 60 N. (a) Experimental alloy, (b) A 309 alloy

surfaces are different for the studied alloy and A 309 alloy; the worn surface consists of plows for the alloy whereas an evident adhesive wear mechanism can be clearly observed for the A 309 alloy (see Fig. 6). At this stage the difference in hardness played a dominant role in determination of wear rate following Archard's law. Therefore, the wear rate of the experimental alloy becomes better than that of A 309 alloy as load increases. The wear resistance of the alloy is three times that of A309 aluminum alloy at high load. Thus, the good wear resistance of the alloy should be related to the high hardness and high compression strength of the alloy.

4. Conclusions

According to above results, adding multicomponent alloying elements under rapid solidification can strengthen aluminum alloy. The effect of the aggrandizement is related to the amount and kind of the alloying elements. The hardness and the compression strength of the $Al_{90}Ni_{2.5}Ti_{2.5}La_{2.5}Mn_{2.5}$ alloys reach 285 HV and 712 Mpa, respectively. The alloy exhibits good wear resistance, which is three times that of the conventional A309 aluminum alloy. The high strength and wear resistance of the alloy are attributed to the second-phase strengthening and the solid solution strengthening mechanisms.

Acknowledgment

The financial support from NNSFC (Grant No. 50571040) and "985 Project" of Jilin University are acknowledged.

References

1. R.W. Cahn, Aluminium-Based Glassy Alloys, *Nature*, 1989, **341**, p 183–184
2. A. Inoue, Amorphous, Nanoquasicrystalline and Nanocrystalline Alloys in Al-Based Systems, *Prog. Mater. Sci.*, 1998, **43**, p 365–517
3. Y. He, S.J. Poon, and G.J. Shiflet, Synthesis and Properties of Metallic Glasses that Contain Aluminum, *Science*, 1988, **241**, p 1640–1641
4. A. Inoue, Stabilization of Metallic Supercooled Liquid and Bulk Amorphous Alloys, *Acta Mater.*, 2000, **48**, p 279–306
5. I. Borner and J. Eckert, Phase Formation and Properties of Mechanically Alloyed Amorphous $Al_{85}Y_8Ni_5Co_2$, *Scrip. Mater.*, 2001, **45**, p 237–244
6. I. Manna, P. Nandi, B. Bandyopadhyay, K. Ghoshray, and A. Ghoshray, Microstructural and Nuclear Magnetic Resonance Studies of Solid-State Amorphization in Al-Ti-Si Composites Prepared by Mechanical Alloying, *Acta Mater.*, 2004, **52**, p 4133–4142
7. I. Mannay, P. Nandi, and P.M.G. Nambissanz, Mechanism and Kinetics of Solid-State Amorphization by Mechanical Alloying of Al65Cu352xNbx, *Philos. Mag.*, 2004, **84**, p 3585–3598
8. G.M. Dougherty, G.J. Shiflet, and S.J. Poon, Synthesis and Microstructural Evolution of Al-Ni-Fe-Gd Metallic Glass by Mechanical Alloying, *Acta Mater.*, 1994, **42**, p 2275–2283
9. A. Inoue, S. Sobu, D.V. Louzguine, H. Kimura, and K. Sasamori, Ultrahigh Strength Al-Based Amorphous Alloys Containing Sc, *J. Mater. Res.*, 2004, **19**, p 1539–1543
10. Y. Kawamura, H. Mano, and A. Inoue, Nanocrystalline Aluminum Bulk Alloys with a High Strength of 1420 MPa Produced by the Consolidation of Amorphous Powders, *Scripta Mater.*, 2001, **44**, p 1599–1604
11. M. Watanabe and A. Inoue, High Mechanical Strength of Rapidly Solidified Al92Mn6Ln2 (Ln = Lanthanide Metal) Alloys with Finely Mixed Icosahedral and Al Phases, *Mater. Trans. JIM*, 1993, **34**, p 162–168
12. M. Takagi, H. Ohta, T. Imura, and A. Inoue, Wear Properties of Nanocrystalline Aluminum Alloys and Their Composites, *Scripta Mater.*, 2001, **44**, p 2145–2152
13. F. Schurack, J. Eckert, and L. Schultz, Quasicrystalline Al-Alloys with High Strength and Good Ductility, *Mater. Sci. Eng. A*, 2000, **294–296**, p 164–167
14. R. Manaila, D. Macovei, R. Popescu, A. Devenyi, A. Jianu, E. Vasile, P.B. Barna, and J.L. Labar, Nano-Icosahedral Al-Mn-Ce Phases: Structure and Local Configurations, *Mater. Sci. Eng. A*, 2000, **294–296**, p 82–85
15. H. Adachi, K. Osamura, S. Ochiai, J. Kusui, and K. Yokoe, Mechanical Property of Nanoscale Precipitate Hardening Aluminum Alloys, *Scripta Mater.*, 2001, **44**, p 1489–1492
16. T. Mukai and K. Higashi, Ductility Enhancement of Ultra Fine-Grained Aluminum Under Dynamic Loading, *Scripta Mater.*, 2001, **44**, p 1493–1496
17. F. Schurack, J. Eckert, and L. Schultz, Synthesis and Mechanical Properties of Cast Quasicrystal-Reinforced Al-Alloys, *Acta Mater.*, 2001, **49**, p 1351–1361
18. G.S. Choi, Y.H. Kim, H.K. Cho, A. Inoue, and T. Masumoto, Ultrahigh Tensile Strength of Amorphous Al-Ni-(Nd,Gd)-Fe Alloys Containing Nanocrystalline Al Particles, *Scripta Metall.*, 1995, **33**, p 1301–1306
19. R. Sabet-Sharghi, Z. Altounian, and W.B. Muir, Formation, Structure, and Crystallization of Al-Rich Metallic Glasses, *J. Appl. Phys.*, 1994, **75**, p 4438–4441
20. R.I. Wu, G. Wilde, and J.H. Perepezko, Glass Formation and Primary Nanocrystallization in Al-Base Metallic Glasses, *Mater. Sci. Eng. A*, 2001, **301**, p 12–17
21. Z.K. Zhao, J.C. Li, and Q. Jiang, Effect of Sintering Temperatures on the Room Temperature Properties of Al90Ce2Mn8 Alloys, *J. Mater. Eng. Perform.*, 2002, **11**, p 262–264
22. J.C. Li, Z.K. Zhao, and Q. Jiang, Properties of High Strength Al85La10Ni5 Alloy, *Mater. Sci. Eng. A*, 2003, **339**, p 205–208
23. C.Y. Xu, S.S. Jia, and Z.Y. Cao, Synthesis of Al-Mn-Ce Alloy by the Spark Plasma Sintering, *Mater. Char.*, 2005, **54**, p 394–398
24. J.C. Li, Q. Jiang, and D.W. Xu, Wear Behavior of Al88La7Ni5 Alloy Prepared by Powder Metallurgy, *Mater. Sci. Technol.*, 2006, **22**, p 604–606
25. J.W. Yeh, S.K. Chen, S.J. Lin, J.Y. Gan, T.S. Chin, T.T. Shun, C.H. Tsau, and S.Y. Chang, Nanostructured High-Entropy Alloys with Multiple Principal Elements: Novel Alloy Design Concepts and Outcomes, *Adv. Eng. Mater.*, 2004, **6**, p 299–303
26. J.W. Yeh, S.K. Chen, J.Y. Gan, S.J. Lin, T.S. Chin, T.T. Shun, C.H. Tsau, and S.Y. Chang, Formation of Simple Crystal Structure in Cu-Co-Ni-Al-Fe-Ti-V Alloys with Multiprincipal Metallic Elements, *Metall. Mater. Trans. A*, 2004, **35**, p 2533–2536
27. B. Cantor, I.T.H. Chang, P. Knight, and A.J.B. Vincent, Microstructural Development in Equiatomic Multicomponent Alloys, *Mater. Sci. Eng. A*, 2004, **375–377**, p P213–P218
28. P.K. Huang, J.W. Yeh, T.T. Shun, and S.K. Chen, Multi-Principal-Element Alloys with Improved Oxidation and Wear Resistance for Thermal Spray Coating, *Adv. Eng. Mater.*, 2004, **6**, p 74–78